

# FLOW TO LEARN: FLOW MATCHING ON NEURAL NETWORK PARAMETERS

Daniel Saragih<sup>\*1</sup> Deyu Cao<sup>1,2,†</sup> Tejas Balaji<sup>1,†</sup> Ashwin Santhosh<sup>1</sup>

<sup>1</sup>University of Toronto    <sup>2</sup>University of Tokyo

## ABSTRACT

Foundational language models show a remarkable ability to learn new concepts during inference via context data. However, similar work for images lag behind. To address this challenge, we introduce FLoWN, a flow matching model that learns to generate neural network parameters for different tasks. Our approach models the flow on latent space, while conditioning the process on context data. Experiments verify that FLoWN attains various desiderata for a meta-learning model. In addition, it matches or exceeds baselines on in-distribution tasks, provides better initializations for classifier training, and is performant on out-of-distribution few-shot tasks while having a fine-tuning mechanism to improve performance.

## 1 INTRODUCTION

Flow matching (FM) (Albergo & Vanden-Eijnden, 2023; Lipman et al., 2023; Liu et al., 2023) is a prominent fixture in generative modeling tasks from imaging (Lipman et al., 2023; Tong et al., 2024; Esser et al., 2024; Liu et al., 2024b) to language (Gat et al., 2024; Shaul et al., 2024; Campbell et al., 2024). However, its application to neural network weights has not been explored. By leveraging the principled, yet versatile training of FM, we aim to generate task-specific weights on novel tasks.

Multiple approaches have been tried to generate weights capable of few-shot learning (FSL), motivated by its speed compared to conventional training. For instance, various diffusion-based approaches (Soro et al., 2024; Zhang et al., 2024; Wang et al., 2024) have been used to generate neural network weights. However, flexibility is limited by its restriction to Gaussian processes and a sluggish inference speed. More broadly, we may categorize this form of learning as meta-learning (Fifty et al., 2024; Hu et al., 2022b; Zhmoginov et al., 2022), which aims to learn concepts from a few demonstrations. It is therefore natural that we have two evaluation settings: in-distribution tasks and out-of-distribution (OOD) tasks. With enough training and capacity, it’s clear *meta-models* (i.e. models trained on multiple data distributions) should excel at in-distribution tasks. However, generalization to novel tasks often presents a challenge to meta-learning and weight generation frameworks (Wang et al., 2024; Schürholt et al., 2024). Recently, Soro et al. (2024) goes to some extent to cross this generalization gap, however, we show that some improvements can be made to the approach. See Appendix A.1 for further related works.

In this paper, we introduce Flow-based Learning of Weights for Neural adaptation (FLoWN), a new class of method for weight generation. Empirical evaluations validate the following contributions: **1)** The generated weights match or exceed conventionally trained models on in-distribution tasks, and provide better initializations for fine-tuning on OOD tasks, **2)** FLoWN is able to conditionally retrieve pre-trained weights from a distribution pre-trained on various datasets while matching their performance, **3)** FLoWN is capable of performing well on OOD few-shot tasks while having a fine-tuning mechanism to improve performance.

<sup>\*</sup>Main correspondence: daniel.saragih@mail.utoronto.ca

<sup>†</sup>Equal contribution

## 2 METHODS

### 2.1 PRELIMINARIES

**Conditional flow models.** Chen et al. (2019) first introduced continuous normalizing flows as an effective data generation process through modeling dynamics. Simulation-free methods improve on this concept by simplifying the training objective (Lipman et al., 2023; Albergo & VandenEijnden, 2023; Liu et al., 2023). Following the formulation of Lipman et al. (2023), given random variables  $\bar{\mathbf{x}}_0 \sim p_0$  and  $\bar{\mathbf{x}}_1 \sim p_1$  a data distribution, define a reference flow  $\bar{\mathbf{x}} = (\bar{\mathbf{x}}_t)_{t \in [0,1]}$  where  $\bar{\mathbf{x}}_t = \beta_t \bar{\mathbf{x}}_0 + \alpha_t \bar{\mathbf{x}}_1$  with the constraint that  $\alpha_0 = \beta_1 = 0$  and  $\alpha_1 = \beta_0 = 1$ . The aim of flow modeling is to learn a sequence  $\mathbf{x} = (\mathbf{x}_t)_{t \in [0,1]}$  which has the same marginal distribution as  $\bar{\mathbf{x}}$ . To make this a feasible task, we describe this process as an ODE:  $d\mathbf{x}_t = v(\mathbf{x}_t, t)dt$  where  $\mathbf{x}_0 \sim \mathcal{N}(0, \mathbf{I})$ . Training proceeds by first parameterizing  $v(\mathbf{x}_t, t)$  by a neural network  $\theta$  and matching the reference flow velocity, i.e.  $u(\mathbf{x}_t, t) := \frac{d}{dt}\bar{\mathbf{x}}_t$ . This would, however, be an unfeasible training objective, therefore, we condition on samples from the terminal distribution  $\mathbf{x}_1 \sim p_1$  and train

$$L_{\text{cfm}}(\theta) = \mathbb{E}_{t \sim U[0,1], \mathbf{x}_1 \sim p_1, \mathbf{x}_t \sim p_t(\cdot | \mathbf{x}_1)} \|v_\theta(\mathbf{x}_t, t) - u(\mathbf{x}_t, t, \mathbf{x}_1)\|. \quad (1)$$

Lipman et al. (2023) proved that this loss produces the same gradients as the marginal loss, thus optimizing it will result in convergence to the reference  $u(\mathbf{x}_t, t)$ . Moreover, we can always marginalize an independent conditioning variable  $\mathbf{y}$  on  $v_\theta, u$  – this will serve as our context conditioning vector.

**Few-shot learning.** The problem of few-shot learning is often formulated as a  $n$ -way- $k$ -shot classification task. In particular, given  $n$  classes and  $k$  examples for each class,  $\mathcal{S} = \{(\mathbf{x}_i, \mathbf{y}_i)\}_{i=1}^{nk}$  of (image, label) *support* set pairs, our meta-learner is tasked with classifying *query* set images  $\mathcal{Q} = \{\mathbf{x}_{nk+1}, \dots, \mathbf{x}_{nk+q}\}$ . Relevant to our approach, recently, Fifty et al. (2024) proposed an image meta-learning architecture, CAML, consisting of three components: a frozen pre-trained image encoder, a class encoder, and a transformer-based sequence model. ELMES, the class encoder, was shown to possess two attractive properties: label symmetry and permutation invariance. The transformer sequence model takes the concatenation of the image and label embeddings of the support set images, and a special "unknown" label embedding is used on query set images. These query images are analogous to the [CLS] tokens in transformers as the logits corresponding to the query images are then passed into a classifier MLP to predict labels.

### 2.2 FLOW TO LEARN

We describe the components of our approach below and leave more details to Appendix A.2, A.3.

**Weight encoder.** Due to the intractable size of weight space, it is necessary for modeling to take place in latent space. We justify this design by appealing to work on the Lottery Ticket Hypothesis (Frankle & Carbin, 2019; Liu et al., 2024a) as well as the body of work on pruning (Cheng et al., 2024), which suggests that, like natural data, neural networks live on a low-dimensional manifold within its ambient space. We use three encoder variants in this paper, first is a variational autoencoder (VAE) (Kingma & Welling, 2022) set up as in Soro et al. (2024), and the second is the graph-based encoder (GE) of Kofinas et al. (2024) which takes into account permutation invariance of neural networks, and third is based on the Learning on LoRAs (LoL) architecture (Putterman et al., 2024). Usage of each variant is dependent on experimental settings.

**Flow meta-model.** The backbone of our meta-learning framework is a conditional FM model following Tong et al. (2024). We make use of the flexibility of FM to use a non-Gaussian prior, specifically the Kaiming uniform or normal initializations (He et al., 2015b), as the source  $p_0$ . The data distribution  $p_1$  of base model weights is experiment-dependent, however, broadly they are obtained by conventional training methods or through a model zoo (Schürholt et al., 2022).

**Conditioning model.** To condition our flow meta-model, we use a pre-trained CAML (Fifty et al., 2024) adapted by Low-rank adaptation modules (LoRAs) (Hu et al., 2022a). Our choice is due to the extensive training of the CAML architecture on several datasets as well as the principled label encoding used in their approach. As we are only interested in an overall encoding of support images, we append a combining layer to aggregate the image latents. The conditioning vector is incorporated by concatenating to the latent vector.

Table 1: Best validation accuracy of unconditional FLoWN generation. *orig* denotes base models trained conventionally and *p-diff* those generated using p-diff (Wang et al., 2024).

Base Models	CIFAR100			CIFAR10			MNIST			STL10		
	orig.	FLoWN	p-diff.	orig.	FLoWN	p-diff.	orig.	FLoWN	p-diff.	orig.	FLoWN	p-diff.
Resnet-18	71.45	71.42	71.40	94.54	94.36	94.36	99.68	99.65	99.65	62.00	62.00	62.24
ViT-base	85.95	85.86	85.85	98.20	98.11	98.12	99.41	99.38	99.36	96.15	95.77	95.80
ConvNext-tiny	85.06	85.12	85.17	98.03	97.89	97.90	99.42	99.41	99.40	95.95	95.63	95.63
CNN w/ VAE	32.09	31.36	30.67	72.53	69.97	69.18	98.93	98.91	98.93	53.88	53.50	53.86
CNN w/ GE	32.09	31.73	31.81	72.53	72.15	72.09	98.93	98.89	98.89	53.88	53.64	53.80

### 3 EXPERIMENTS

First, we confirm various properties that are to be expected of weight generation models. Next, we examine FLoWN’s performance in few-shot learning. Further details are provided in A.4.

#### 3.1 BASIC PROPERTIES OF FLoWN

**Unconditional generation.** We first evaluate the basic modeling capabilities of the flow meta-model. The target distribution  $p_1$  is generated by training a variety of base models on known datasets: CIFAR10, CIFAR100, and MNIST, and saving 200 weight checkpoints each. For large models, we can choose to generate only a subset of the weights. In our case, we generate the batch norm parameters for ResNet-18 (He et al., 2015a), ViT-base (Dosovitskiy et al., 2021) and ConvNext-tiny (Liu et al., 2022), and the full medium-CNN (Schürholt et al., 2022). The aim of this test is to train a separate meta-model for each dataset and validate its base model reconstruction on classifying its corresponding test set. Table 1 shows that we are able to match base models trained conventionally and with p-diff (Wang et al., 2024).

Table 2: Mean validation accuracy of top-5 FLoWN model retrievals, one with a mini-Imagenet prior.

Method	MNIST	F-MNIST	CIFAR10	STL10
Original	91.1	72.7	48.7	39.0
FLoWN w/ mIN-prior	63.0	41.9	22.6	18.8
FLoWN	91.7	73.8	50.3	40.8

Table 3: Mean validation accuracy of fine-tuned generated weights post-retrieval. The asterisk (\*) indicates datasets on which the model was not trained.

Epoch	Method	MNIST	F-MNIST	CIFAR10	STL10	USPS*	SVHN*	KMNIST*
0	RandomInit	~ 10%	~ 10%	~ 10%	~ 10%	~ 10%	~ 10%	~ 10%
	FLoWN	83.58 ± 0.58	68.50 ± 0.64	45.93 ± 0.57	35.16 ± 1.24	57.53 ± 2.43	17.99 ± 0.82	11.79 ± 0.51
1	RandomInit	18.12 ± 1.58	26.90 ± 0.52	28.75 ± 0.22	18.94 ± 0.09	17.69 ± 0.00	19.50 ± 0.03	14.48 ± 0.06
	FLoWN	84.49 ± 0.65	69.09 ± 0.40	46.85 ± 0.30	36.15 ± 1.14	72.45 ± 1.81	68.64 ± 7.07	51.15 ± 8.90
5	RandomInit	35.05 ± 3.87	51.08 ± 2.15	40.00 ± 0.20	28.24 ± 0.01	32.77 ± 0.46	39.59 ± 10.0	30.00 ± 0.30
	FLoWN	87.68 ± 0.44	70.32 ± 0.50	47.44 ± 0.55	37.43 ± 1.19	76.96 ± 1.29	77.36 ± 1.07	69.14 ± 10.1
25	RandomInit	87.70 ± 0.90	70.69 ± 0.46	46.86 ± 0.01	36.75 ± 0.10	82.02 ± 0.12	58.56 ± 19.5	55.05 ± 0.06
	FLoWN	92.29 ± 0.41	73.72 ± 0.68	49.25 ± 0.73	40.14 ± 1.07	82.28 ± 1.40	78.75 ± 1.30	79.11 ± 6.65
50	RandomInit	92.76 ± 0.08	72.88 ± 0.46	48.85 ± 0.74	40.47 ± 0.18	88.35 ± 0.18	63.70 ± 22.1	64.32 ± 0.25

**Model retrieval and in-distribution initialization.** Following (Soro et al., 2024), we perform model retrieval to test whether the meta-model can distinguish weights of the base model given conditioning samples from the dataset the base model was trained on. The base model is a simple 4-layer ConvNet and we obtain 100 weight checkpoints from the model zoo (Schürholt et al., 2022) for each dataset: MNIST, Fashion-MNIST (F-MNIST), CIFAR10, and STL10 after 46-50 epochs of conventional training. Unlike in the previous test, we will train just a single meta-model on 400 total base models conditioned on support samples from their training set via CAML. During validation, we pass in a random support sample from one of the four datasets and generate the *full* ConvNet. In Table 2, we see that our top-5 validation accuracy matches that of the base models. Additionally, we repeated this experiment using weights from mini-Imagenet as a prior, but they seem to perform considerably worse than just Kaiming normal (see A.4.2 for a discussion). Next, we repeat this experiment but instead using weight checkpoints from epochs 21-25, and use the generated weights as an initialization before fine-tuning another 25 epochs. As shown in Table 3, our initialization

enjoys faster convergence, even for datasets on which the model was not trained, highlighting the generalization capability of our meta-model.

### Fine-tuning the meta-model on OOD data.

The setting of unconditional generation is quite restrictive as it is assumed that the output classifier has the same architecture and is to be used on the same dataset. In this experiment, we evaluate whether the meta-model can be effectively fine-tuned to achieve better performance on out-of-distribution data. We start with the meta-model trained from unconditional generation and generate weights for a different dataset. Subsequently, we compute the cross-entropy loss and backpropagate the gradients through the FM model. As this entails back-propagation through an ODE solver, we implement a stopgrad mechanism that restricts gradient flow before a time  $0 < t' < 1$  to trade off accuracy for efficiency. Due to time constraints, we restrict ourselves to batch norms of ResNet-18 and the small-CNN. Table 4 shows considerable improvement over generations obtained from a static FM meta-model and the VAE.

Table 4: Fine-tuning on OOD data. Data-F are results generated from fine-tuned meta-models, whereas Data-S are from static meta-models. Here, we generate the full CNN weights, whereas we only modify the batch norms of ResNet-18.

Base dataset	ResNet-18		CNN w/ VAE		CNN w/ GE	
	CIFAR10	STL10	CIFAR10	STL10	CIFAR10	STL10
CIFAR10-S	-	64.20	-	24.01	-	23.03
CIFAR10-F	-	72.87	-	60.09	-	60.85
STL10-S	93.09	-	19.97	-	18.13	-
STL10-F	94.06	-	61.38	-	69.42	-

## 3.2 FEW-SHOT LEARNING

For this evaluation, we use mini-Imagenet (Vinyals et al., 2016) and a pre-trained ResNet-12 (Chen et al., 2021). Following the typical FSL setting, the dataset is partitioned into meta-train and meta-test sets, and further into tasks whose size depends on the way and shot parameters. For instance, for 5-way-1-shot, the support set consists of one image from 5 classes, whereas the query set is always 15 images for each of the 5 classes in the support set. The in-distribution test entails labeling query images from the same dataset (i.e. trained on mini-Imagenet and evaluated on mini-Imagenet), whereas OOD tasks entail labeling novel query images. First, we train the ResNet-12 on the train split of mini-Imagenet; our goal is thus to generate a classifier head for each task.

In our case, we set 50,000 tasks in the meta-train set and 100 in the meta-test set. We perform this test by constructing a target distribution using pre-trained weights from ResNet-12, linear-probing a classifier head on top of the ResNet backbone for each of the 50,000 subsets for 100 epochs using the AdamW optimizer with a learning rate of  $10^{-3}$  and weight decay of  $10^{-2}$ . Given our computational constraints, we evaluated FLoWN on just two out-of-distribution datasets: CIFAR10 and STL10 by sampling weights 50 different times and taking the average top-3 accuracies. Table 5 shows that our method achieves marginal gains on CIFAR10, but performance on STL10 remains below the baseline. Considering the high validation accuracies of our VAE, we anticipate that further training and tinkering, which we plan to conduct in subsequent revisions, will enhance FLoWN generalization across tasks.

Table 5: Few-shot learning accuracy on out-of-distribution tasks. We compare with D2N WG and best reconstruction of the classifier weights by our out-of-distribution VAE.

Model	CIFAR10	STL10
Max acc. VAE Recon.	<b>73.1</b>	<b>80.4</b>
D2N WG (Soro et al., 2024)	33.04 ± 0.04	50.42 ± 0.13
FLoWN	51.46 ± 8.02	56.24 ± 8.96

## 4 DISCUSSION AND FUTURE WORK

In this work, we have provided a preliminary investigation of FLoWN for weight generation with an application to few-shot learning. Future research directions include: **1)** training FLoWN on a more comprehensive image dataset to improve efficacy on OOD tasks, **2)** a post-hoc fine-tuning mechanism (Domingo-Enrich et al., 2024) for adapting FLoWN to difficult domains (e.g. medical imaging), **3)** incorporating intermediate base model weights obtained during conventional training to guide the inference trajectory of generated weights (e.g. via MetricFM (Kapusniak et al., 2024)).

## ACKNOWLEDGMENTS

The authors would like to thank Lazar Atanackovic and Kirill Neklyudov for helpful discussions in the planning stages and later discussions of the manuscript.

## REFERENCES

- Michael Samuel Albergo and Eric Vanden-Eijnden. Building normalizing flows with stochastic interpolants. In *The Eleventh International Conference on Learning Representations*, 2023. URL <https://openreview.net/forum?id=li7qeBbCR1t>.
- Antreas Antoniou, Harrison Edwards, and Amos Storkey. How to train your MAML. In *International Conference on Learning Representations*, 2019. URL <https://openreview.net/forum?id=HJGven05Y7>.
- Jacob Beck, Matthew Thomas Jackson, Risto Vuorio, and Shimon Whiteson. Hypernetworks in Meta-Reinforcement Learning. In *Proceedings of The 6th Conference on Robot Learning*, pp. 1478–1487. PMLR, March 2023.
- Andrew Campbell, Jason Yim, Regina Barzilay, Tom Rainforth, and Tommi Jaakkola. Generative flows on discrete state-spaces: Enabling multimodal flows with applications to protein co-design. *arXiv preprint arXiv:2402.04997*, 2024.
- Ricky T. Q. Chen, Yulia Rubanova, Jesse Bettencourt, and David Duvenaud. Neural Ordinary Differential Equations, December 2019.
- Yinbo Chen, Zhuang Liu, Huijuan Xu, Trevor Darrell, and Xiaolong Wang. Meta-baseline: Exploring simple meta-learning for few-shot learning. In *Proceedings of the IEEE/CVF International Conference on Computer Vision*, pp. 9062–9071, 2021.
- Hongrong Cheng, Miao Zhang, and Javen Qinfeng Shi. A survey on deep neural network pruning: Taxonomy, comparison, analysis, and recommendations. *IEEE Transactions on Pattern Analysis and Machine Intelligence*, 46(12):10558–10578, 2024. doi: 10.1109/TPAMI.2024.3447085.
- Tarin Clanuwat, Mikel Bober-Irizar, Asanobu Kitamoto, Alex Lamb, Kazuaki Yamamoto, and David Ha. Deep learning for classical japanese literature, 2018.
- Adam Coates, Andrew Ng, and Honglak Lee. An analysis of single-layer networks in unsupervised feature learning. In *AISTATS*, 2011.
- Gabriele Corso, Luca Cavalleri, Dominique Beaini, Pietro Liò, and Petar Veličković. Principal neighbourhood aggregation for graph nets, 2020. URL <https://arxiv.org/abs/2004.05718>.
- Misha Denil, Babak Shakibi, Laurent Dinh, Marc’Aurelio Ranzato, and Nando de Freitas. Predicting Parameters in Deep Learning, October 2014.
- Cameron Diao and Ricky Loynd. Relational attention: Generalizing transformers for graph-structured tasks. In *The Eleventh International Conference on Learning Representations*, 2023. URL <https://openreview.net/forum?id=cFuMmbWiN6>.
- Carles Domingo-Enrich, Michal Drozdal, Brian Karrer, and Ricky T. Q. Chen. Adjoint Matching: Fine-tuning Flow and Diffusion Generative Models with Memoryless Stochastic Optimal Control, September 2024.
- Alexey Dosovitskiy, Lucas Beyer, Alexander Kolesnikov, Dirk Weissenborn, Xiaohua Zhai, Thomas Unterthiner, Mostafa Dehghani, Matthias Minderer, Georg Heigold, Sylvain Gelly, Jakob Uszkoreit, and Neil Houlsby. An image is worth 16x16 words: Transformers for image recognition at scale. In *International Conference on Learning Representations*, 2021. URL <https://openreview.net/forum?id=YicbFdNTTy>.
- Yingjun Du, Zehao Xiao, Shengcai Liao, and Cees Snoek. ProtoDiff: Learning to Learn Prototypical Networks by Task-Guided Diffusion, November 2023.

- Patrick Esser, Sumith Kulal, Andreas Blattmann, Rahim Entezari, Jonas Müller, Harry Saini, Yam Levi, Dominik Lorenz, Axel Sauer, Frederic Boesel, Dustin Podell, Tim Dockhorn, Zion English, Kyle Lacey, Alex Goodwin, Yannik Marek, and Robin Rombach. Scaling rectified flow transformers for high-resolution image synthesis, 2024. URL <https://arxiv.org/abs/2403.03206>.
- Christopher Fifty, Dennis Duan, Ronald G. Jenkins, Ehsan Amid, Jure Leskovec, Christopher Re, and Sebastian Thrun. Context-Aware Meta-Learning, March 2024.
- Chelsea Finn, Pieter Abbeel, and Sergey Levine. Model-Agnostic Meta-Learning for Fast Adaptation of Deep Networks. In *Proceedings of the 34th International Conference on Machine Learning*, pp. 1126–1135. PMLR, July 2017.
- Jonathan Frankle and Michael Carbin. The lottery ticket hypothesis: Finding sparse, trainable neural networks. In *International Conference on Learning Representations*, 2019. URL <https://openreview.net/forum?id=rJl-b3RcF7>.
- Itai Gat, Tal Remez, Neta Shaul, Felix Kreuk, Ricky T. Q. Chen, Gabriel Synnaeve, Yossi Adi, and Yaron Lipman. Discrete flow matching. In *The Thirty-eighth Annual Conference on Neural Information Processing Systems*, 2024. URL <https://openreview.net/forum?id=GTDKo3Sv9p>.
- David Ha, Andrew M. Dai, and Quoc V. Le. Hypernetworks. In *International Conference on Learning Representations*, 2017.
- Kaiming He, X. Zhang, Shaoqing Ren, and Jian Sun. Deep residual learning for image recognition. *2016 IEEE Conference on Computer Vision and Pattern Recognition (CVPR)*, pp. 770–778, 2015a. URL <https://api.semanticscholar.org/CorpusID:206594692>.
- Kaiming He, Xiangyu Zhang, Shaoqing Ren, and Jian Sun. Delving deep into rectifiers: Surpassing human-level performance on imagenet classification. In *2015 IEEE International Conference on Computer Vision (ICCV)*, pp. 1026–1034, 2015b. doi: 10.1109/ICCV.2015.123.
- Edward J Hu, yelong shen, Phillip Wallis, Zeyuan Allen-Zhu, Yanzhi Li, Shean Wang, Lu Wang, and Weizhu Chen. LoRA: Low-rank adaptation of large language models. In *International Conference on Learning Representations*, 2022a. URL <https://openreview.net/forum?id=nZevKeeFYf9>.
- Shell Xu Hu, Da Li, Jan Stühmer, Minyoung Kim, and Timothy M. Hospedales. Pushing the Limits of Simple Pipelines for Few-Shot Learning: External Data and Fine-Tuning Make a Difference, April 2022b.
- J.J. Hull. A database for handwritten text recognition research. *IEEE Transactions on Pattern Analysis and Machine Intelligence*, 16(5):550–554, 1994. doi: 10.1109/34.291440.
- Kacper Kapusniak, Peter Potapchik, Teodora Reu, Leo Zhang, Alexander Tong, Michael Bronstein, Avishek Joey Bose, and Francesco Di Giovanni. Metric Flow Matching for Smooth Interpolations on the Data Manifold, May 2024.
- Diederik P Kingma and Max Welling. Auto-encoding variational bayes, 2022. URL <https://arxiv.org/abs/1312.6114>.
- Louis Kirsch, James Harrison, Jascha Sohl-Dickstein, and Luke Metz. General-purpose in-context learning by meta-learning transformers, 2024. URL <https://arxiv.org/abs/2212.04458>.
- Miltiadis Kofinas, Boris Knyazev, Yan Zhang, Yunlu Chen, Gertjan J. Burghouts, Efstratios Gavves, Cees G. M. Snoek, and David W. Zhang. Graph Neural Networks for Learning Equivariant Representations of Neural Networks. <https://arxiv.org/abs/2403.12143v3>, March 2024.
- A. Krizhevsky and G. Hinton. Learning multiple layers of features from tiny images. *Master’s thesis*, 2009.

- Jonathan Lee, Annie Xie, Aldo Pacchiano, Yash Chandak, Chelsea Finn, Ofir Nachum, and Emma Brunskill. Supervised Pretraining Can Learn In-Context Reinforcement Learning. *Advances in Neural Information Processing Systems*, 36:43057–43083, December 2023.
- Yaron Lipman, Ricky T. Q. Chen, Heli Ben-Hamu, Maximilian Nickel, and Matt Le. Flow Matching for Generative Modeling, February 2023.
- Bohan Liu, Zijie Zhang, Peixiong He, Zhensen Wang, Yang Xiao, Ruimeng Ye, Yang Zhou, Wei-Shinn Ku, and Bo Hui. A survey of lottery ticket hypothesis, 2024a. URL <https://arxiv.org/abs/2403.04861>.
- Xingchao Liu, Chengyue Gong, and qiang liu. Flow straight and fast: Learning to generate and transfer data with rectified flow. In *The Eleventh International Conference on Learning Representations*, 2023. URL <https://openreview.net/forum?id=XVjTT1nw5z>.
- Xingchao Liu, Xiwen Zhang, Jianzhu Ma, Jian Peng, and qiang liu. InstafLOW: One step is enough for high-quality diffusion-based text-to-image generation. In *The Twelfth International Conference on Learning Representations*, 2024b. URL <https://openreview.net/forum?id=1k4yZbbDqX>.
- Zhuang Liu, Hanzi Mao, Chao-Yuan Wu, Christoph Feichtenhofer, Trevor Darrell, and Saining Xie. A convnet for the 2020s, 2022. URL <https://arxiv.org/abs/2201.03545>.
- Yuval Netzer, Tao Wang, Adam Coates, Alessandro Bissacco, Bo Wu, and Andrew Y. Ng. Reading digits in natural images with unsupervised feature learning. In *NIPS Workshop on Deep Learning and Unsupervised Feature Learning 2011*, 2011. URL [http://ufldl.stanford.edu/housenumbers/nips2011\\_housenumbers.pdf](http://ufldl.stanford.edu/housenumbers/nips2011_housenumbers.pdf).
- Aram-Alexandre Pooladian, Heli Ben-Hamu, Carles Domingo-Enrich, Brandon Amos, Yaron Lipman, and Ricky T. Q. Chen. Multisample flow matching: straightening flows with minibatch couplings. In *Proceedings of the 40th International Conference on Machine Learning, ICML’23*. JMLR.org, 2023.
- Marcin Przewieźlikowski, Paweł Przybyś, Jacek Tabor, Maciej Zieba, and Przemysław Spurek. Hypermaml: Few-shot adaptation of deep models with hypernetworks. *ArXiv*, abs/2205.15745, 2022.
- Theo Putterman, Derek Lim, Yoav Gelberg, Stefanie Jegelka, and Haggai Maron. Learning on lorax: G<sub>L</sub>-equivariant processing of low-rank weight spaces for large finetuned models, 2024. URL <https://arxiv.org/abs/2410.04207>.
- Aravind Rajeswaran, Chelsea Finn, Sham M. Kakade, and Sergey Levine. *Meta-learning with implicit gradients*. Curran Associates Inc., Red Hook, NY, USA, 2019.
- Sachin Ravi and Hugo Larochelle. Optimization as a Model for Few-Shot Learning. In *International Conference on Learning Representations*, February 2017.
- Konstantin Schürholt, Diyar Taskiran, Boris Knyazev, Xavier Giró-i Nieto, and Damian Borth. Model zoos: A dataset of diverse populations of neural network models. In *Thirty-Sixth Conference on Neural Information Processing Systems (NeurIPS) Track on Datasets and Benchmarks*, September 2022.
- Konstantin Schürholt, Michael W. Mahoney, and Damian Borth. Towards scalable and versatile weight space learning. In *Proceedings of the 41st International Conference on Machine Learning (ICML)*. PMLR, 2024.
- Neta Shaul, Itai Gat, Marton Havasi, Daniel Severo, Anuroop Sriram, Peter Holderrieth, Brian Karrer, Yaron Lipman, and Ricky T. Q. Chen. Flow matching with general discrete paths: A kinetic-optimal perspective, 2024. URL <https://arxiv.org/abs/2412.03487>.
- Bedionita Soro, Bruno Andreis, Hayeon Lee, Song Chong, Frank Hutter, and Sung Ju Hwang. Diffusion-based Neural Network Weights Generation, February 2024.

- Alexander Tong, Kilian Fatras, Nikolay Malkin, Guillaume Huguet, Yanlei Zhang, Jarrid Rector-Brooks, Guy Wolf, and Yoshua Bengio. Improving and generalizing flow-based generative models with minibatch optimal transport, March 2024.
- Oriol Vinyals, Charles Blundell, Timothy Lillicrap, koray kavukcuoglu, and Daan Wierstra. Matching networks for one shot learning. In D. Lee, M. Sugiyama, U. Luxburg, I. Guyon, and R. Garnett (eds.), *Advances in Neural Information Processing Systems*, volume 29. Curran Associates, Inc., 2016. URL [https://proceedings.neurips.cc/paper\\_files/paper/2016/file/90e1357833654983612fb05e3ec9148c-Paper.pdf](https://proceedings.neurips.cc/paper_files/paper/2016/file/90e1357833654983612fb05e3ec9148c-Paper.pdf).
- Kai Wang, Zhaopan Xu, Yukun Zhou, Zelin Zang, Trevor Darrell, Zhuang Liu, and Yang You. Neural Network Diffusion, February 2024.
- Ross Wightman. Pytorch image models. <https://github.com/rwightman/pytorch-image-models>, 2019.
- Han Xiao, Kashif Rasul, and Roland Vollgraf. Fashion-mnist: a novel image dataset for benchmarking machine learning algorithms, 2017.
- Baoquan Zhang, Chuyao Luo, Demin Yu, Xutao Li, Huiwei Lin, Yunming Ye, and Bowen Zhang. Metadiff: Meta-learning with conditional diffusion for few-shot learning. *Proceedings of the AAAI Conference on Artificial Intelligence*, 38(15):16687–16695, Mar. 2024.
- Dominic Zhao, Seijin Kobayashi, João Sacramento, and Johannes von Oswald. Meta-Learning via Hypernetworks. In *4th Workshop on Meta-Learning at NeurIPS 2020 (MetaLearn 2020)*. NeurIPS, December 2020. doi: 10.3929/ethz-b-000465883.
- Andrey Zhmoginov, Mark Sandler, and Max Vladymyrov. HyperTransformer: Model Generation for Supervised and Semi-Supervised Few-Shot Learning, July 2022.

## A APPENDIX

This appendix consist of details left out in the main text. First, we perform a more comprehensive review of the related literature with further discussion of our motivations. Next, we go over the various components of FLoWN and expound on their implementation and training procedure.

### A.1 RELATED WORKS

**Conditional flow matching.** The CFM objective, where a conditional vector field is regressed to learn probability paths from a source to target distribution, was first introduced in Lipman et al. (2023). The CFM objective attempts to minimize the expected squared loss of a target conditional vector field (which is conditioned on training data and generates a desired probability path) and an unconditional neural network. The authors showed that optimizing the CFM objective is equivalent to optimizing the unconditional FM objective. Moreover, the further work (Tong et al., 2024) highlighted that certain choices of parameters for the probability paths led to the optimal conditional flow being equivalent to the optimal transport path between the initial and target data distributions, thus resulting in shorter inference times. However, the original formulations of flow matching assumed that the initial distributions were Gaussian. Pooladian et al. (2023) extended the theory to arbitrary source distributions using minibatch sampling and proved a bound on the variance of the gradient of the objective. Tong et al. (2024) showed that using the 2-Wasserstein optimal transport map as the joint probability distribution of the initial and target data along with straight conditional probability paths results in a marginal vector field that solves the dynamical optimal transport problem between the initial and target distributions.

**Neural network parameter generation.** Due to the flexibility of neural network as function approximators, it is natural to think that they could be applied to neural network weights. Denil et al. (2014) paved the way for this exploration as their work provided evidence of the redundancy of most network parameterizations, hence showing that parameter generation is a feasible objective. Later, Ha et al. (2017) introduced Hypernetworks which use embeddings of weights of neural network

layers to generate new weights and apply their approach to dynamic weight generation of RNNs and LSTMs. A significant portion of our paper’s unconditional parameter generation section builds upon the ideas from Wang et al. (2024) and the concurrent work of Soro et al. (2024) where the authors employ a latent diffusion model to generate new parameters for trained image classification networks.

**Meta-learning context.** Although neural networks are adept at tasks on which they were trained, a common struggle of networks is generalization to unseen tasks. In contrast, humans can often learn new tasks when given only a few examples. A pioneering modern work in this field is MAML (Finn et al., 2017), which learns good initialization parameters for the meta-learner such that it can easily be fine-tuned to new tasks. Their approach utilizes two nested training loops. The inner loop computes separate parameters adapted to each of the training tasks. The outer loop computes the loss using each of these parameters on their respective tasks and updates the model’s parameters through gradient descent. However, MAML often had unstable training runs, and so successive works gradually refined the method (Antoniou et al., 2019; Rajeswaran et al., 2019; Zhao et al., 2020; Przewieźlikowski et al., 2022). The aforementioned works typically focus on classification tasks, however, this paradigm allows for great versatility. For instance, Beck et al. (2023) used hypernetworks to generate the parameters of a policy model and (Lee et al., 2023) exploited the in-context learning ability of transformers to general reinforcement learning tasks.

**Weight generation for few-shot learning.** Following up on the work of meta-learning context, few-shot learning is a natural application of such meta-learning algorithms. An early example is Ravi & Larochelle (2017) who designed a meta-learner based on the computations in an LSTM cell. At each training example in the support set, their meta learner uses the losses and the gradients of the losses of the base learner (in addition to other information from previous training examples) to produce base learner parameters for the next training example. The loss of the base learner on the test examples in the support set is backpropagated through the meta learner’s parameters. Moreover, we may leverage the advancements in generative modeling for weight generation. As we mentioned, Lee et al. (2023) used transformers for in-context reinforcement learning, but we also see the works of Zhmoginov et al. (2022); Hu et al. (2022b); Kirsch et al. (2024); Fifty et al. (2024) use transformers and foundation models. More similar to our method is the body of work on using diffusion models for weight generation (Du et al., 2023; Zhang et al., 2024; Wang et al., 2024; Soro et al., 2024). These methods vary in their approach, some leveraging a relationship between the gradient descent algorithm and the denoising step in diffusion models to design their meta-learning algorithm. Others rely on the modeling capabilities of conditioned latent diffusion models to learn the target distribution of weights. Most evaluations conducted were in-distribution tasks, i.e. tasks sampled from the same data distribution as the training tasks, hence, there is room to explore ways of adapting this approach for out-of-distribution tasks.

## A.2 ARCHITECTURE DETAILS

Here, we expound on the architecture of FLoWN. See Figure 1 for a schematic of the training and inference process.

### A.2.1 VARIATIONAL AUTOENCODER

The variational autoencoder follows the implementation of Soro et al. (2024). In particular, given a set of model weights  $\{\mathcal{M}_i\}_{i=1}^N$ , we first flatten the weights to obtain vectors  $\mathbf{w}_i \in \mathbb{R}^{d_i}$ . For the sake of uniformity, we always zero-pad vectors to  $d = \max_i d_i$ . Alternatively, we allow for layer-wise vectorization: set a chunk size  $\ell$  which corresponds to the weight dimension of a network layer. Then, zero-pad  $\mathbf{w}_i$  to be a multiple of  $\ell$ , say  $\tilde{d}$ . This allows us to partition into  $k$  equal length vectors  $\mathbf{w}_{i,k} \in \mathbb{R}^{\tilde{d}/k}$ . Typically, larger models benefit from layer-wise vectorization.

Subsequently, we train a VAE to obtain an embedding of such vectors by optimizing the objective:

$$L_{\text{VAE}}(\theta, \phi) := -\mathbb{E}_{\mathbf{z} \sim q(\mathbf{z}|\mathbf{w})} [\log p_{\theta}(\mathbf{w}|\mathbf{z}) + \beta D_{KL}(q_{\phi}(\mathbf{z}|\mathbf{w})||p(\mathbf{z}))] \quad (2)$$

where  $\mathbf{w}$  is the vectorized weights,  $\mathbf{z}$  is the embedding we are learning, and  $p_{\theta}, q_{\phi}$  are the reconstruction and posterior distributions respectively. Moreover, we fix the prior  $p(\mathbf{z})$  to be a  $(0, 1)$ -Gaussian

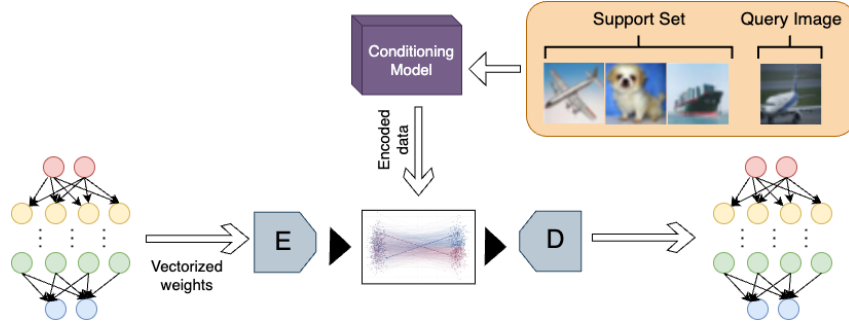


Figure 1: A schematic of the training process of FLoWN for few-shot learning. Given a set of pre-trained target weights and a support set, we apply the conditioned flow model to pushforward a sample of the latent prior towards encoded target weights. The decoder is used during inference where we start from a sample of the latent prior and pushforward towards the target distribution with a trained vector field  $v_\theta(\cdot, t; \mathbf{y})$  where  $\mathbf{y}$  is the support set embedding.

and the weight is set to be  $\beta = 10^{-2}$ . For layer-wise vectorization, we simply change the input dimensions to match the chunk size. Upon decoding, we concatenate the chunks to re-form the weight vector.

#### A.2.2 GRAPH ENCODER

Recently, Kofinas et al. (2024) proposed a neural graph encoder which incorporates the permutation invariance present in network weights. The method has two components: a graph constructor and the embedding model. The neural network is first represented as a graph where nodes represent the neurons within each network layer and edges represent neuronal connections. Importantly, node features correspond to bias parameters and edge features correspond to weight parameters. Subsequently, this is fed into an embedding model, such as a GNN, specifically PNA (Corso et al., 2020), or a relational transformer (Diao & Loynd, 2023). For our use case, we outline weights-to-graphs conversion of MLPs, CNNs, and normalization layers. See Kofinas et al. (2024) for more details.

**MLPs to graphs.** Let  $\mathcal{G}(\mathbf{V}, \mathbf{E})$  be a graph and let the vertex set  $\mathbf{V} \in \mathbb{R}^{n \times d_V}$  and the adjacency matrix  $\mathbf{E} \in \mathbb{R}^{n \times n \times d_E}$ . Intuitively, if we have  $n$  nodes in a graph, our vertex set is size  $n$ , and the adjacency matrix is  $n \times n$ . In our case, we also incorporate node and edge features, hence an extra dimension is added. Consider an  $L$ -layer MLP with weights  $\{\mathbf{W}^\ell \in \mathbb{R}^{d_\ell \times d_{\ell-1}}\}_{\ell=1}^L$  and biases  $\{\mathbf{b}^\ell \in \mathbb{R}^{d_\ell}\}_{\ell=1}^L$ . Since we have a node for each neuron, we have  $n = \sum_{\ell=0}^L d_\ell$ , where  $d_0$  is the input dimension. Now, let’s use these to construct the vertex set  $\mathbf{V}$ . Since each neuron has a corresponding bias term (except the input),  $\mathbf{V} = [\mathbf{0}_{d_0} \ \mathbf{b}^1 \ \dots \ \mathbf{b}^L]^\top$ . As for the adjacency matrix, consider the first  $d_0$  rows: as this corresponds to the input layer, it’s only connected to the first layer, i.e. only columns  $d_0 + 1$  to  $d_0 + d_1$  are possibly non-zero. And if we focus on row  $i \in [d_0]$ , what are its features? They must be  $\mathbf{W}_{:,i}^1$ . Hence,

$$(\mathbf{E}_{[0:d_0] \times [d_0+1, d_0+d_1]})^\top = \mathbf{W}^1,$$

and elsewhere in  $\mathbf{E}_{[0:d_0]}$  is zero. In general,

$$(\mathbf{E}_{[d_{i-1}:d_i] \times [d_{i-1}+1, d_{i-1}+d_i]})^\top = \mathbf{W}^i,$$

and is zero everywhere else. In other words, the first off-diagonal blocks are precisely  $\mathbf{W}^i$ , and  $\mathbf{E}$  is zero elsewhere. Finally, what are  $d_E$  and  $d_V$ ? This turns out to be problem-dependent. Sometimes, it helps to add useful node features, but if the only thing we are concerned about embedding is weight information, then each entry of  $\mathbf{W}^i$  and  $\mathbf{b}^i$  is simply a scalar, so  $d_E = d_V = 1$ .

**Normalization layers to graphs.** Either BatchNorm or LayerNorm can be written as  $\mathbf{y} = \mathbf{m} \odot \mathbf{x} + \mathbf{b}$ , where  $\mathbf{m}, \mathbf{x}, \mathbf{b}, \mathbf{y} \in \mathbb{R}^d$ . The trick is to recast this as a linear layer: we can always write  $\mathbf{y} = \text{diag}(\mathbf{m})\mathbf{x} + \mathbf{b}$ . Hence, we ought to have  $d$  nodes for  $\mathbf{x}$  and another  $d$  nodes for  $\mathbf{y}$  where the nodes for  $\mathbf{y}$  have biases  $\mathbf{b}$ . The two layers are then connected by weight matrix  $\text{diag}(\mathbf{m})$  which only connects  $x_i$  to  $y_i$ .

Table 6: Model architectures and hyperparameters. Square brackets  $[\cdot]$  indicates an interval of values. For instance, we often train until a loss plateau, hence the varying number of epochs.

Parameters	Model Retrieval Few-Shot Learning	
<b>Dataset Encoder (Frozen)</b>		
Architecture	CAML	CAML
Latent Dimension	1024	1024
<b>Weight Encoder</b>		
Architecture	VAE	VAE
Latent Space Size	$4 \times 4 \times 4$	$4 \times 8 \times 8$
Upsampling/Downsampling Layers	5	4
Channel Multiplication (per Downsampling Layer)	(1, 1, 2, 2, 2)	(1,1,2,2)
ResNet Blocks (per Layer)	2	2
KL-Divergence Weight	0.01	1e-6
Optimizer	AdamW	AdamW
Learning Rate	$1 \times 10^{-3}$	$1 \times 10^{-2}$
Weight Decay	$2 \times 10^{-6}$	$2 \times 10^{-6}$
Batch Size	32	128
Training Epochs	3000	[100, 500]
<b>Conditional Flow Matching Model</b>		
Timestep and Dataset Embedding Size	128	128
Input Size	$4 \times 4 \times 4$	$4 \times 8 \times 8$
Optimizer	AdamW	AdamW
Learning Rate	$1 \times 10^{-3}$	$2 \times 10^{-4}$
Weight Decay	$2 \times 10^{-6}$	$2 \times 10^{-6}$
Batch Size	32	128
Training Epochs	[3000, 10000]	[100, 500]
NFE	100	100

**CNNs to graphs.** To simplify consider one convolutional layer between layers  $\ell - 1$  and  $\ell$ , namely  $\mathbf{W} \in \mathbb{R}^{d_\ell \times d_{\ell-1} \times w_\ell \times h_\ell}$  and  $\mathbf{b} \in \mathbb{R}^{d_\ell}$ . Intuitively,  $d_{\ell-1}$  is the number of input channels and  $d_\ell$  the number of output channels. Due to the spatial dimension  $w_\ell \times h_\ell$ , we first flatten the last two layers. Now, we make use of the node and edge features: instead of scalar weights like in linear layers, our weights are vectors of size  $w_\ell \times h_\ell$ . However, the size may be different between layers, so we take  $s = (\max_{\ell \in [L]} w_\ell, \max_{\ell \in [L]} h_\ell)$  and zero-pad our weight vectors as necessary before flattening. Hence, following the procedure in the MLP conversion, we form an adjacency matrix with vector features, i.e.  $\mathbf{E} \in \mathbb{R}^{n \times n \times d_E}$  where  $d_E = w_{\max} h_{\max}$ .

### A.2.3 FLOW MODEL

The neural network used for flow matching is the UNet from D2NWX (Soro et al., 2024). The specific hyperparameters used for the CFM model varies between experiments, so we leave this discussion to A.4.

## A.3 TRAINING DETAILS

Here, we present further training and experimental details.

### A.3.1 PRE-TRAINED MODEL ACQUISITION

**Datasets and architectures.** We conduct experiments on a wide range of datasets, including CIFAR-10/100 (Krizhevsky & Hinton, 2009), STL-10 (Coates et al., 2011), (Fashion/K)-MNIST (Xiao et al., 2017; Clanuwat et al., 2018), USPS (Hull, 1994), and SVHN Netzer et al. (2011). To evaluate our meta-model’s ability to generate new subsets of network parameters, we conduct experiments on ResNet-18 (He et al., 2015a), ViT-Base (Dosovitskiy et al., 2021), ConvNeXt-Tiny (Liu et al., 2022), the latter two are sourced from timm Wightman (2019). As we shall detail below, small CNN architectures from a model zoo (Schürholt et al., 2022) are also used for full-model generations.

**Model pre-training.** For better control over the target distribution  $p_1$ , in experiments involving ResNet-18, ViT-Base, and ConvNeXt-Tiny, we pre-train these base models from scratch on their respective datasets. We follow Wang et al. (2024) and train the base models until their accuracy stabilizes. Further, we train the relevant subset (e.g. batch norm parameters for ResNet-18) for another 200 epochs, saving the weights at the end.

**Model zoo.** The model zoo used for meta-training in the model retrieval setting, as described in Sec. 3.1, was sourced from (Schürholt et al., 2022). As the base model, we employed their CNN-small architecture, which consists of three convolutional layers and contains either 2,464 or 2,864 parameters, depending on the number of input channels. For each dataset—MNIST, Fashion-MNIST, CIFAR-10, and STL10—100 sets of pre-trained weights were randomly selected from the model zoo using different seeds and fixed hyperparameters (referred to as "Seed" in their codebase). For the training of base models, we adopted the same hyperparameters as those used in (Schürholt et al., 2022) for all datasets, except KMNIST, which was not included in their model zoo. For KMNIST, we used the hyperparameters applied to MNIST, given the similarity between the two datasets.

### A.3.2 VARIATIONAL AUTOENCODER TRAINING

The VAE was trained with the objective in equation 2. Moreover, following p-diff (Wang et al., 2024), we add Gaussian noise to the input and latent vector, i.e. given noise factors  $\sigma_{in}$  and  $\sigma_{lat}$  with encoder  $f_\phi$  and decoder  $f_\theta$ , we instead have

$$z = f_\phi(w + \xi_{in}), \hat{w} = f_\theta(z + \xi_{lat}) \quad \text{where} \quad \xi_{in} \sim \mathcal{N}(0, \sigma_{in}^2 \mathbf{I}), \xi_{lat} \sim \mathcal{N}(0, \sigma_{lat}^2 \mathbf{I}).$$

A new VAE is trained at every instantiation of the CFM model as architectures often differ in their input dimension for different experiments. However, they are trained with different objectives: the VAE is trained to minimize reconstruction loss. In all experiments, we fix  $\sigma_{in} = 0.001$  and  $\sigma_{lat} = 0.5$ .

### A.3.3 GRAPH ENCODER TRAINING

The graph encoder (Kofinas et al., 2024) was used for both the unconditional generation and fine-tuning on OOD experiments with the CNN-medium architecture from Schürholt et al. (2022). We restricted our tests to the relational transformer (Diao & Loynd, 2023) which was shown to perform better in the original paper (Kofinas et al., 2024). See Table 7 for the instantiation parameters.

### A.4 EXPERIMENTAL DETAILS

In this section, experimental hyperparameter details are given alongside estimates of computation time on an A100 GPU.

#### A.4.1 UNCONDITIONAL GENERATION

Unconditional generation involves two stages: first is the training of base models. We choose a Resnet18, ViT-B, ConvNext-tiny, and medium-CNN for our base models and provide the training parameters in Table 8. Next, is the stage where we train either a AE-CFM or AE-DDPM, with the encoder being the same in both cases; the training parameters for this stage is provided in Table 10. We found that in most cases, the autoencoder and CFM converge after 1000 epochs. In this case, we estimate training time to be between 2-3 hours when the VAE is used. When the graph encoder is used, of course the CFM training time remains the same, however, the encoder takes 6-8 hours of training. Validation requires less than 1 min. to run due to the small latent dimension.

Table 7: Preprocessing and graph encoder hyperparameters.

Parameters	Values
<b>Dataset Preprocessing</b>	
Input Channels	3
Image shape	(32, 32)
$(w_{max}, h_{max})$	(7, 7)
Max. spatial res.	49
Max. # hidden layers	5
Flattening Method	Repeat Nodes
Normalize	False
Augmentation	False
Linear as Conv.	False
<b>Relational Transformer</b>	
Embed dim.	64
Num. layers	4
Num. heads	8
Num. probe features	0

Table 8: Task Training

Parameters	ResNet18	ViT & ConvNext	CNN
Optimizer	SGD	AdamW	AdamW
Initial Training LR	0.1	$1 \times 10^{-4}$	$3 \times 10^{-3}$
Training Scheduler	MultiStepLR	CosineAnnealingLR	CosineAnnealingLR
Layer Weights Saved	Last 2 BN layers	Last 2 BN layers	All layers
Initial Model Saving LR	$1.6 \times 10^{-4}$	$5 \times 10^{-2}$	$1 \times 10^{-3}$
Model Saving Scheduler	None	CosineAnnealingLR	CosineAnnealingLR
Number of Models Saved	200	200	200
Num. of Weights per Model	2048	3072	[10565, 12743]
Training Epochs	100	100	100
Batch Size	64	128	128

#### A.4.2 MODEL RETRIEVAL

The first column of Table 6 shows the details of the model architectures and training configurations. For each dataset, we first generate its CAML embedding by (1) averaging the query image embeddings within each class to get class embeddings, (2) concatenating the class embeddings into one long vector, (3) passing the combined class embeddings through two linear layers to produce the final dataset embedding. Next, the dataset embedding is combined with the timestep embedding via a projection layer, and the resulting representation is used as input to the flow matching model. We estimate a training time of 2 hours for the VAE and 4 hours for the CFM to achieve our level of accuracy. Inference times remain the same as in *unconditional generation*.

A mini-Imagenet prior for CFM. As mentioned in Sec. 3.1, we attempted this experiment with priors from a pre-trained mini-Imagenet. There were a few technical hurdles with the implantation of these weights. First, for 1-channel datasets such as MNIST, the input weight shapes are smaller than those of the mini-Imagenet model. Second, the classification head of a mini-Imagenet model predicts a much greater number of classes than our test datasets. Our procedure is as follows: we train a small-CNN model (Schürholt et al., 2022) on mini-Imagenet until its accuracy stabilizes. Next, we take the mean  $\mu$  and standard deviation  $\sigma$  of its classifier head. Using these statistics, we initialized the classifier heads of our base models as  $\mathcal{N}(\mu, \sigma^2 \mathbf{I})$ . For the rest of the base model, we pad to the prior’s shape if necessary, and we implant the pre-trained weights directly before adding Gaussian  $\mathcal{N}(\mathbf{0}, \mathbf{I})$  noise. Since we flow in latent space, our last step is to apply the VAE to the weights we’ve constructed.

Figure 2 shows the training curve with our mini-Imagenet prior in blue, and with a Gaussian 0-1 prior in orange. It is striking that the loss decreases much faster, but as seen in Table 2, the test accuracies are quite poor. This points to an issue such as overfitting, which is likely caused by latent space capacity. Indeed, with our approach of constructing the prior, we invoke the VAE encoder twice: once to encode the prior and once more to encode the target weights. The target weights were those pre-trained on one of the four datasets in Table 2, hence it’s expected that the distribution is quite distinct from those pre-trained on mini-Imagenet. Due to the size of our latent space (64, as noted in Table 6), it may be insufficient to encode both distributions. Moreover, the loss objective for encoding the prior is not ideal. As the encoder is invoked in forward passes of the CFM, it only learns how to encode the prior such that CFM loss decreases, as opposed to a reconstruction objective. Hence, future work could look to modify encoder training so as to reconstruct both target weights and weights of the prior.

Table 9: Finetuning

Parameters	ResNet18	CNN
Optimizer	AdamW	AdamW
Num Epochs	[50,100]	[50, 100]
Initial LR	$1 \times 10^{-2}$	$1 \times 10^{-5}$
Detach Value	0.4	0.4
LR Scheduler	None	CosineAnnealingLR
Minimum LR	$1 \times 10^{-2}$	$5 \times 10^{-7}$

#### A.4.3 FEW-SHOT LEARNING

For the few-shot learning experiments, we adopted the same methodology for obtaining dataset embeddings and conditioning parameter generation as in the model retrieval experiment. Classifier

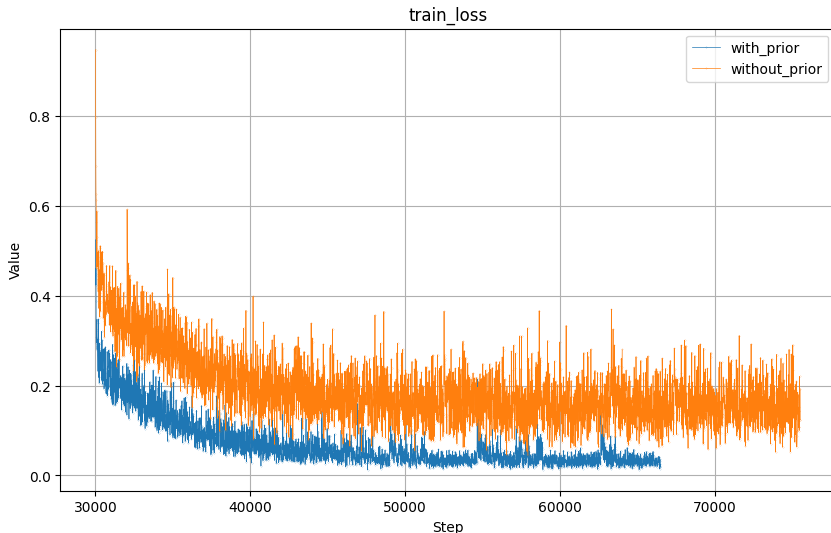


Figure 2: The training loss curve for the mini-Imagenet run from Table 2.

Table 10: CFM/DDPM

Parameters	AE CFM	AE DDPM
Flow/Diffusion Optimizer	AdamW	AdamW
Flow/Diffusion LR	0.001	0.001
Autoencoder Optimizer	AdamW	AdamW
Num Inference Timesteps	100	[100, 1000]
Autoencoder LR	0.001	0.001
Weight Initialization	Kaiming	Normal
Autoencoder Epochs	[1000, 30000]	[1000, 30000]
CFM/DDPM Epochs	[1000, 30000]	[1000, 30000]
Batch Size	[50, 200]	[50, 200]

heads were trained on 50,000 randomly sampled 5-way 1-shot subsets of the mini-ImageNet dataset (Vinyals et al., 2016), and the resulting pre-trained weights were used as training data for the meta-model. The hyperparameter configurations for meta-training are provided in the second column of Table 6. During evaluation, we measured the accuracies of the generated models on two out-of-distribution datasets, CIFAR-10 and STL-10. For each subset, we sampled 50 sets of weights and reported the average accuracy of the top three performing models. We estimate a training time of 4 hours for the VAE (until convergence) and 7 hours of CFM training until convergence.

#### A.4.4 FINE-TUNING ON OUT-OF-DISTRIBUTION DATA

We provide the hyperparameters of the fine-tuning experiment in Table 9. The computational cost of this experiment mainly lie in the backpropagation step through the ODE solver used for CFM inference. We implemented a `stopgrad` mechanism to trade off efficiency for accuracy, and this parameter was set to detach the computation graph at  $t = 0.4$ , therefore saving 40% of backpropagation had we not used it. The total runtime depends on the dataset used, but we estimate a runtime of about 16 hours.